Research Square

Preprints are preliminary reports that have not undergone peer review.
They should not be considered conclusive, used to inform clinical practice,
or referenced by the media as validated information.

Tobacco callus as a novel bioproduction platform for β-ionone synthesis via carotenoid cleavage dioxygenases

Fan Li
Shaanxi Institute of Microbiology
Xu Zhang
Shaanxi Institute of Microbiology
Jun Wang
Shaanxi Institute of Microbiology
SiNan Chen
Shaanxi Institute of Microbiology
YueJuan Zhang
Shaanxi Institute of Microbiology
XiuLin Han
Yunnan University
MengLiang Wen
Yunnan University
XiaoWei Gong
R&D Center of China Tobacco Yunnan Industrial Co., Ltd
Ying Mao
National Nonferrous Metals Product Quality Inspection and Testing Center (Yunnan)
Yi Wan
wanyi65650163.com

Shaanxi Institute of Microbiology

Research Article

Keywords: βCarotene, Carotenoid cleavage dioxygenases, β-Ionone, Tobacco callus

Posted Date: October 23rd, 2026

DOI: https://doi.org/10.21203/rs.3.rs-11185978/v1

License: This work is licensed under a Creative Commons Attribution 4.0 International License.
Read Full License

Additional Declarations: No competing interests reported.

Abstract

β-Ionone is a high-value C13-norisoprenoid that contributes floral and woody notes to tobacco products. Although microbial platforms can produce β-ionone, they rely on complex heterologous engineering and energy-intensive downstream processing, which raise costs and hinder direct application. Here, we explored tobacco callus as an alternative, homologous production chassis that exploits the plant's endogenous carotenoid pool. We expressed the tobacco carotenoid cleavage dioxygenases NtCCD4 and NtCCD10 in stable transgenic callus lines, achieving de novo β-ionone synthesis at 0.96 and 0.54 μg/g dry weight, respectively. The engineered tissue was directly incorporated into heated tobacco products without extraction, where it enhanced aroma complexity and imparted a moist, sweet aftertaste. This study establishes tobacco callus as a novel, low-cost green-manufacturing platform for tobacco-derived flavour compounds and demonstrates the direct in-planta application of engineered biomass in tobacco products.

Key message

Tobacco callus engineered with NtCCD4/NtCCD10 produces β-ionone in situ and can be directly used in heated tobacco products as a green, low-cost flavour platform.

1 Introduction

β-Ionone, a monocyclic C13-norisoprenoid, is a high-value aroma compound prized for its distinctive floral, woody and fruity notes. It is widely used in personal-care and household fragrance products, and it also exhibits notable pharmacological activities, including anti-inflammatory and anticancer effects (Dong et al. 2019). Furthermore, β-ionone is classified as generally recognized as safe (GRAS) by FEMA and approved by the U.S. FDA (Lalko et al. 2007), which supports its use in flavours and fragrances and underpins its growing market value.

In plants, β-ionone is synthesized through the mevalonate (MVA) and methylerythritol phosphate (MEP) pathways (Fig. 1). These pathways originate from acetyl-CoA and D-glyceraldehyde-3-phosphate, respectively, and converge at geranylgeranyl diphosphate (GGPP). GGPP is converted to β-carotene by geranylgeranyl diphosphate synthase (crtE), phytoene synthase/cyclase (crtYB) and phytoene desaturase (crtI). Finally, β-carotene is cleaved by carotenoid cleavage dioxygenases (CCDs) to yield β-ionone; the CCD-catalysed step is the key rate-limiting reaction in this pathway.

CCDs comprise a diverse enzyme family, including the CCD1, CCD2, CCD4, CCD7, CCD8 and CCD10 subfamilies, each with distinct functional properties. Whereas CCD1 and CCD4 show broad substrate specificity, cleaving several carotenoids at different double-bond positions (Morote et al. 2023; Qi et al. 2023; Yoo et al. 2023; Ke et al. 2025), CCD2 is highly specific for zeaxanthin at the 7,8 (7',8') conjugated double bond (Ahrazem et al. 2016; Fang et al. 2020). CCD7 and CCD8 mainly participate in strigolactone biosynthesis (Chen et al. 2023; Yi et al. 2023), whereas CCD10, a recently characterized subfamily,

cleaves β-carotene at the 9,10 (9',10') position (Wang et al. 2019; Zhong et al. 2020; Fan et al. 2022). Notably, CCD1, CCD4 and CCD10 are the main enzymes responsible for β-ionone formation.

As an inherent aroma compound in tobacco, β-ionone strongly influences leaf quality; nevertheless, research on tobacco CCDs remains limited. Our previous work identified eight CCD genes in *Nicotiana tabacum* cultivar K326 and classified them into the CCD1, CCD4 and CCD10 subfamilies (Gong et al. 2022). Because tobacco naturally accumulates carotenoid precursors, we hypothesized that tobacco callus could serve as a direct platform for β-ionone production without precursor supplementation.

In contrast to microbial systems, which often require exogenous precursor feeding or co-expression of multiple heterologous enzymes—leading to metabolic burden and regulatory complexity (Zhang et al. 2018; Werner et al. 2019)—plant cell cultures offer distinct advantages. Tobacco callus harbours an endogenous precursor pool, grows on simple and low-cost media, and aligns with the principles of green biomanufacturing (Efferth 2019). Moreover, because the engineered callus can be incorporated directly into heated tobacco products without downstream extraction or purification, it avoids aroma loss and removes the need for artificial additives.

In this study, we selected NtCCD4 and NtCCD10 as candidate genes on the basis of their predicted roles in β-ionone synthesis. After bioinformatic analysis and functional validation in Escherichia coli, both genes were transiently expressed in *N. benthamiana* for subcellular localization. Stable overexpression in tobacco callus achieved β-ionone synthesis at 0.96 and 0.54 μg/g dry weight (DW), respectively. When incorporated directly into heated tobacco products, the engineered callus enhanced aroma complexity and imparted a moist, sweet aftertaste. These results show that tobacco callus is a novel bioproduction platform for β-ionone, enabling in situ synthesis and direct application in next-generation tobacco products.

2 Materials and methods

2.1 Strains and reagents

The strains used in this study are listed in Table S1. *Escherichia coli* Top10 was used for plasmid construction, and *Agrobacterium tumefaciens* LBA4404 (maintained in our laboratory) was used for tobacco callus transformation.

β-Ionone and β-carotene were purchased from Sigma-Aldrich (St. Louis, MO, USA). Ampicillin, kanamycin, rifampicin, chloramphenicol, hygromycin and cefotaxime were obtained from Macklin (Shanghai, China; https://www.macklin.cn/) and dissolved in water to the required concentrations. 1-Naphthylacetic acid (NAA), indole-3-acetic acid (IAA), kinetin (KT) and 6-benzylaminopurine (BAP) were prepared in ethanol; 2,4-dichlorophenoxyacetic acid (2,4-D), vitamins (B1, B3, B6) and Murashige & Skoog (MS) medium were purchased from Shanghai Yuanye Bio-Technology (https://shyuanye.com/) and prepared in water.

2.2 Medium and cultivation conditions

Luria–Bertani (LB) medium was used to culture *E. coli* and *A. tumefaciens* for plasmid extraction, protein expression and seed activation. MS1–MS4 media were used to induce tobacco callus. When required, the medium was supplemented with 50 μg/mL ampicillin, 50 μg/mL kanamycin, 25 μg/mL rifampicin, 50 μg/mL chloramphenicol, 50 μg/mL hygromycin or 200 μg/mL cefotaxime.

2.3 Strains and plasmid construction

Plasmids, primers and sequences of the genetic parts are listed in Tables S2, S3 and S4, respectively. The pCold TF plasmid was used for protein expression, pAC-BETAXipi for β-carotene production, and pCAMBIA1301 for CCD expression. The *CCD* genes from *N. tabacum* cultivar K326 (NtCCD4, GenBank NM_001325517.1; NtCCD10, GenBank XM_016626693) were codon-optimized for tobacco, synthesized by Tsingke Biotechnology (Tianjin, China), and cloned into the *Eco*R I and *Kpn* I sites of pCold TF. The 1301-NtCCD10 plasmid was generated by seamless cloning of four fragments—the 35S promoter and NOS terminator (from pCAMBIA1301), the *NtCCD10* gene (from the NtCCD10-TF plasmid) and the *GFP* gene (from pGFP)—and the assembled cassette was inserted into the *Eco*R I site of pCAMBIA1301. The 1301-NtCCD4 plasmid was constructed by seamless cloning of four fragments—the 35S promoter, NOS terminator (PCR-amplified from pCAMBIA1301), mCherry (from p2300) and the *NtCCD4* gene (from NtCCD4-TF)—and inserted into the *Pma*C I and *Nco* I sites of pCAMBIA1301.

The caroCCDs-TOP10 strain was constructed by co-transforming pAC-BETAXipi and CCDs-TF into *E. coli* Top10. The LBA4404-CCDs strains were constructed by transforming 1301-NtCCD4 and 1301-NtCCD10 separately into *A. tumefaciens* LBA4404, following the method of Gelvin (2003).

2.4 Culture conditions

All experiments were performed in biological triplicate. The caroCCDs-TOP10 strain was cultured in LB with antibiotics at 37°C until the optical density at 600 nm (OD600) reached 0.6–0.8. Protein expression was induced with 1.0 mM isopropyl β-D-1-thiogalactopyranoside (IPTG) using a two-stage temperature shift: 24 h at 15°C followed by 24 h at 28°C. Cells were harvested, sonicated and extracted with n-hexane; the organic phase was concentrated, redissolved in dodecane, filtered and analysed by HPLC. The LBA4404-CCDs strain was cultured in LB with antibiotics (50 μg/mL kanamycin, 25 μg/mL rifampicin) to OD600 1.0, harvested, resuspended in MMA buffer (10 mM MgCl2, 10 mM MES, 100 μM acetosyringone, pH 5.8) to OD600 1.0, and incubated at room temperature for 3–4 h before vacuum infiltration of leaves.

Seeds of *N. benthamiana* were sown in pots containing a 1:3 mixture of zirconium beads and potting soil. Plants were grown at 26°C under a 16 h light/8 h dark photoperiod, with a light intensity of 70 μmol m^{-2} s^{-1} and ~ 60% relative humidity. Leaves from 4–5-week-old plants were collected for callus induction.

2.5 Tobacco callus induction and transformation

Tobacco callus induction was performed based on Lang et al. (2020) with modifications. For leaf-disc transformation, discs from 4–5-week plants were immersed in recombinant Agrobacterium for 5 min, rinsed with sterile water containing 200 μg/mL cefotaxime, and co-cultured on MS4 medium in darkness at 26°C. After 48 h, explants were transferred to MS4 medium containing hygromycin (50 μg/mL) and cefotaxime (200 μg/mL) until callus formation. In pre-induced transformation, leaf discs were pre-cultured for 1–2 weeks until swollen tissue formed; for callus transformation, pre-formed callus pieces were used directly for infection. Both methods followed the same subsequent steps as leaf-disc transformation.

2.6 Bioinformatics analysis

Multiple sequence alignment of the proteins was performed using the BIC web server (https://www.bic.ac.cn/Cloud_Platform/front/) for alignment visualization. Three-dimensional structures were predicted with AlphaFold2 and visualized with PyMOL 3.0. Substrate channels were analysed with Caver Web (https://loschmidt.chemi.muni.cz/caverweb/). Subcellular localization was predicted with Cell-PLoc-2 (http://www.csbio.sjtu.edu.cn/bioinf/Cell-PLoc-2/).

2.7 Detection methods

HPLC analysis was performed on an Agilent 1260 system equipped with an XTerra RP18 column (5 μm, 3.9 × 150 mm). The mobile phase was isopropanol and 80% acetonitrile at a flow rate of 0.5 mL/min, column temperature 30°C, injection volume 10 μL, detection wavelength 219 nm and total run time 50 min.

β-Ionone was quantified by UPLC–MS/MS according to the method of Mi et al. (2018), with quantification based on external standard curves.

2.8 Processing of tobacco products

Granular core substrates for heated tobacco products were prepared by screw extrusion–spheronization. A mixture of 50 g tobacco-leaf powder, 20 g aerosol former, 12.5 g water and 4 g engineered callus was conditioned for 2 h, extruded (1.0 mm die, 45 rpm), spheronized (1500 rpm, 3 min) and dried (90°C, 40 min). Pellets (180 mg) were assembled into cigarettes with defined segment lengths (Fig. S1) using 6000 CU tipping paper.

2.9 Statistical analysis

Data are presented as mean ± standard deviation (SD) with at least three biological replicates unless stated otherwise. Statistical analyses were performed with GraphPad Prism v8 and Excel 2010 (Microsoft, Redmond, WA, USA). Significance was assessed by one-way analysis of variance (ANOVA) with Tukey's test; bars labelled with different lowercase letters indicate significant differences at $P < 0.001$.

3 Results and discussion

3.1 Protein analysis of NtCCD4 and NtCCD10

On the basis of our analysis of tobacco *CCD* genes, we selected NtCCD4 and NtCCD10 for β-ionone production. The two enzymes differ markedly in amino-acid sequence (Fig. 2A, black pentagram vs. triangle), reflecting their distinct subfamily classification and characteristic motifs (Fig. 2B), which likely underlie their divergent catalytic properties and substrate preferences.

To explore the structural basis of the predicted functional divergence, we modelled their three-dimensional structures and substrate channels. The substrate-channel locations in both models were consistent with previous reports (Messing et al. 2010), confirming high reliability. The NtCCD10 channel is longer and less curved than that of NtCCD4, and the radius at its narrowest point also differs (Table 1, Fig. 2B). We reasoned that, for long-chain polyene substrates such as β-carotene, a longer, less-curved channel may facilitate entry and binding of the linear molecule, thereby enhancing catalytic efficiency. On this structural basis, we predicted that NtCCD10 would outperform NtCCD4 in β-ionone synthesis.

Table 1
Substrate channel evaluation of candidate proteins.

Protein	Length (Å)	Curvature	Bottleneck radius (Å)	Distance to surface (Å)
NtCCD4	32.8	1.7	1.3	19.6
NtCCD10	40.1	1.3	1.4	21.6

Subcellular localization also influences catalytic efficiency. Our predictions placed NtCCD4 in plastids and NtCCD10 in the cytoplasm, consistent with the known localization of other CCDs. Because the precursor β-carotene is synthesized in plastids, NtCCD4 would benefit from spatial proximity and thus higher catalytic efficiency—the opposite of the structural prediction. These conflicting observations reveal a trade-off between intrinsic activity and substrate accessibility in vivo, so the better enzyme in tobacco callus had to be determined experimentally.

3.2 Functional validation of CCDs in *E.coli*

To verify the function of NtCCD4 and NtCCD10, they were cloned and co-transformed with the β-carotene synthesis plasmid pAC-BETAXipi into *E. coli* Top10 (Fig. 3A).

Compared with the control (CaroTF-TOP10) and the β-carotene-producing strain (Caro-TOP10), the co-transformed strains (CaroCCDs-TOP10) showed visibly lighter coloration (Fig. 3B), suggesting consumption of β-carotene. Consistently, β-carotene yields in Caro-TOP10, CaroTF-TOP10, CaroNtCCD4-TOP10 and CaroNtCCD10-TOP10 were 5.43, 5.35, 0.40 and 0.66 mg/g DW, respectively (Fig. 3C). The β-carotene content in Caro-TOP10 and CaroTF-TOP10 was significantly higher than in the CCD-expressing strains, confirming that NtCCD4 and NtCCD10 efficiently degrade β-carotene.

β-Ionone yields in the control strains (Caro-TOP10 and CaroTF-TOP10) were 0.27 and 0.29 mg/g DW, respectively, attributed to non-enzymatic auto-oxidative cleavage of β-carotene under the in vitro

conditions. β-Ionone yields in CaroNtCCD4-TOP10 and CaroNtCCD10-TOP10 were 3.30 and 3.20 mg/g DW, respectively (Fig. 3C). The two strains showed comparable activity in *E. coli*, in line with previous reports on other CCDs (Meng et al. 2019). Their amino-acid and localization differences did not translate into functional differences in this heterologous host, because the absence of organellar compartments in *E. coli* removes the effect of substrate spatial accessibility on efficiency.

3.3 Subcellular localization of CCDs

To verify the subcellular localization of NtCCD4 and NtCCD10 in planta, transient expression assays were performed in *N. benthamiana*.

We constructed the 1301-NtCCD4 and 1301-NtCCD10 expression vectors (Fig. 4A), with both genes placed under the control of a double CaMV 35S promoter. NtCCD4 was fused in-frame to an mCherry marker via a short linker, whereas NtCCD10 was fused to GFP. Both constructs were introduced into *Agrobacterium tumefaciens* strain LBA4404 and used for agroinfiltration of *N. benthamiana* leaves. Fluorescence was observed at 3 days post-infiltration (dpi). NtCCD4-mCherry co-localized completely with the chloroplast marker (Fig. 4B), confirming plastid localization of NtCCD4. NtCCD10-GFP was distributed at the cell periphery, consistent with cytoplasmic localization. This result matches the bioinformatic prediction and the characteristic localization of the CCD10 subfamily (Dhar et al. 2020).

3.4 Establishment of the tobacco callus

The auxin/cytokinin ratio and concentration are key determinants of callus induction and differentiation (Husin et al. 2005). To identify the most suitable medium, we compared induction efficiency and callus status across four formulations (MS1–MS4, Table 2).

Table 2
Composition of tobacco callus induction media.

Medium	Phytohormone composition	Vitamins & other additives
MS1	IAA 0.5 mg/L; BAP 2 mg/L	—
MS2	KT 0.1 mg/L; 2,4-D 1 mg/L	—
MS3	KT/NAA 0.5/2 mg/L; 2,4-D 1 mg/L	—
MS4	IAA 2 mg/L; 2,4-D 1 mg/L; KT 0.2 mg/L	VB1 0.4, VB3 0.5, VB6 0.5 mg/L

MS1 induced irregular tissue and promoted organogenesis rather than stable callus, making it unsuitable. MS2 and MS3 formed callus from young stem segments but showed high shoot differentiation, prolonged induction and low efficiency (Fig. 5). By contrast, MS4 rapidly produced callus with nearly 100% induction within 2 weeks. We attribute this to an auxin/cytokinin ratio in MS4 that effectively suppressed organ differentiation and promoted rapid, uniform proliferation. Besides phytohormones, B-group vitamins (B1, B3, B6) in MS4 may also promote callus growth by acting as coenzymes in central metabolism (Xinliang 2023).

3.5 Synthesis of β-ionone in tobacco callus

Three transformation methods were compared for conversion efficiency to establish an efficient, stable transformation system (Fig. S2).

In leaf-disc transformation, callus could be induced but grew poorly, appearing loose and white. In pre-induced transformation, callus growth stagnated, probably because Agrobacterium infection damaged early callus cells. The callus-transformation method caused browning and inactivation, possibly owing to residual Agrobacterium and disruption of the microenvironment. These results indicate that pre-induced leaf discs and newly formed callus are too fragile to withstand infection (Nakajima et al. 2020), so the leaf-disc method is the most convenient and effective. Under fluorescence illumination, the NtCCD4 and NtCCD10 lines showed red and green fluorescence, respectively (Fig. 6A); corresponding fluorescence was also observed in dispersed suspension cells (Fig. 6B), confirming *CCDs* expression.

To detect β-carotene, CCD-expressing and wild-type callus were given 48 h light treatment followed by extraction (Fig. S3). Extract colour differed: wild type appeared yellowish, whereas NtCCD4 and NtCCD10 extracts showed a greenish tint (Fig. 7A, B). β-Carotene yields in wild type, NtCCD4 and NtCCD10 were 1.45, 0.45 and 0.63 μg/g DW, respectively (Fig. 7C), consistent with the colour differences. Although wild-type callus also contained carotenoids, levels were low because callus was induced in the dark. The transgenic lines showed even lower β-carotene because CCD overexpression consumed the substrate.

β-Ionone was then extracted and analysed for the NtCCD4 and NtCCD10 lines (Fig. S4). Yields in wild type, NtCCD4 and NtCCD10 were 0.24, 0.96 and 0.54 μg/g DW, respectively (Fig. 7D). The low wild-type value may reflect endogenous CCD activity. No β-ionone was detected in leaf discs before induction, consistent with metabolic reprogramming during phytohormone-mediated callus initiation (Verma et al. 2022). Both transgenic lines produced more β-ionone than wild type, demonstrating the feasibility of β-ionone production in tobacco callus and providing new insight into CCD-mediated biosynthesis.

Notably, in contrast to *E. coli*, NtCCD4 produced more β-ionone than NtCCD10 in tobacco callus. This difference arises from their distinct subcellular localizations and underscores a key advantage of plant-cell systems: spatial substrate access can outweigh intrinsic catalytic differences. This study is the first to demonstrate β-ionone biosynthesis in tobacco callus, highlighting the potential of plant-cell platforms for efficient CCD expression and the production of complex natural products.

3.6 Application of callus in tobacco products

To evaluate the application potential of β-ionone-producing tobacco callus, we tested it in heated cigarettes (Fig. S5).

Processability is a key indicator for practical use in novel tobacco products. The engineered callus showed excellent processability, enabling smooth extrusion and uniform spherical particles because of its homogeneous cell structure, moderate water content and lack of lignified fibres, which facilitate standardized production.

In sensory evaluation, the core substrate containing engineered callus significantly enhanced aroma complexity and imparted a moist, sweet aftertaste relative to the control (Table 3, Fig. S5). β-Ionone contributes characteristic floral and woody notes and effectively modifies the smoke profile while increasing sweetness. Importantly, the aroma-producing callus was mixed directly into the core substrate without extraction, purification or exogenous addition. This avoids loss of volatile aroma compounds during conventional flavour addition and eliminates solvents or carriers, aligning with clean-label and reduced-harm trends in tobacco products.

Table 3
Sensory quality evaluation results of pellet-type heated cigarettes.

Evaluation parameter	WT	NtCCD4	NtCCD10
Smoke yield	+	+	+
Smoke strength	+ +	+ +	+ +
Aroma intensity	+ +	+	+
Aroma complexity	+	+ + +	+ + +
Aftertaste quality	+	+ + +	+ + +
Smoothness	-	+ +	+ + +
Sweet note	-	+ +	+ + +

Note: “—” indicates barely detectable/subdued; “+” indicates moderate/discernible; “++” indicates distinct; “+++” indicates pronounced.

More importantly, this study validates the practical use of a plant-cell chassis. Unlike microbial systems, tobacco callus as a homologous platform retains the product directly in the biomass. This concept applies not only to β-ionone but also to other high-value tobacco-derived flavours. Although the current yield requires improvement, this work is the first to use tobacco callus as a synthesis platform, paving the way for plant-cell factories in the tobacco industry.

3.7 Considerations for improving β-ionone productivity in tobacco callus

Although the engineered callus validates the concept, the attained β-ionone titers (0.96 and 0.54 μg/g DW for NtCCD4 and NtCCD10, respectively) are about three orders of magnitude lower than those reached in the *E. coli* platform (3.30 and 3.20 mg/g DW). This gap does not invalidate the plant-cell approach; rather, it mainly reflects differences in precursor supply and cellular context, and it points to concrete engineering levers.

The dominant bottleneck is precursor availability. In callus, total β-carotene was only 0.45–0.63 μg/g DW, whereas the engineered *E. coli* accumulated 5.43 mg/g DW—a smaller carotenoid pool in the plant host. The endogenous MVA/MEP flux in dark-grown callus is low and is not directed toward carotenoids. In

plants, the “push” strategy of overexpressing upstream enzymes—especially phytoene synthase (PSY), a rate-limiting step—has dramatically increased carotenoid accumulation; for example, Golden Rice 2 reached up to 23-fold higher carotenoids (maximum 37 μg/g) by using a more efficient maize PSY (Paine et al. 2005). Co-overexpressing PSY with carotenoid desaturases/cyclases and silencing competing branches can redirect flux and could raise the β-carotene pool in callus by orders of magnitude (Roberts 2007; Rao and Ravishankar 2002).

Subcellular compartmentalization and substrate accessibility impose a second constraint. β-Carotene is synthesized and sequestered in plastids; plastid-localized NtCCD4 is therefore co-compartmentalized with its substrate, whereas cytosolic NtCCD10 must draw β-carotene (or its cleavage products) across the plastid envelope. This explains why NtCCD4 outperformed NtCCD10 in planta despite the opposite structural prediction, and shows that spatial substrate access outweighs intrinsic catalytic differences in plant cells. Retargeting CCD10 to plastids (via a transit peptide) or co-localizing CCDs with carotenoid-binding proteins, and balancing relative expression so cleavage keeps pace with precursor synthesis, should improve efficiency.

A third lever is enzyme catalytic efficiency. CCDs are slow, membrane-associated dioxygenases whose turnover limits flux. Directed evolution and rational engineering of CCDs have already improved β-ionone yields in yeast (Werner et al. 2019; Gong et al. 2022); porting such optimized variants into callus, or screening NtCCD paralogs and orthologs, could raise per-enzyme productivity. Product stability also matters: β-ionone is volatile and may be further metabolized or conjugated, so net accumulation depends on both synthesis and stability. In situ trapping or sequestration and harvest at the flux optimum can reduce losses.

Finally, host and process engineering can deliver scalable supply. Plant cell cultures are established platforms for high-value metabolites and can be scaled in bioreactors; commercial successes such as paclitaxel from Taxus cell cultures show that initially low titers can be raised to industrially relevant levels through elicitation, in situ product removal and metabolic engineering (Wilson and Roberts 2012; Rao and Ravishankar 2002). Selecting high-producing callus lines and moving to suspension cultures would improve biomass productivity and uniformity relative to the current solid callus. Because the biomass is used directly, even moderate per-gram titers may be acceptable if the feedstock is cheap and scalable—the platform’s value lies in its grow-and-use loop.

In summary, this study establishes tobacco callus as a viable, low-cost and green chassis for in situ β-ionone production and its direct application in next-generation tobacco products. The current yield is a starting point constrained mainly by precursor supply and subcellular compartmentalization, and it is addressable through precursor-pathway engineering, enzyme optimization and process scale-up. Future work should quantify carbon flux through the MVA/MEP and carotenoid pathways in callus and implement the strategies outlined above, positioning plant-cell factories as a complementary route to microbial biosynthesis for tobacco-derived flavour compounds.

Abbreviations

2,4-D	2,4-dichlorophenoxyacetic acid
BAP	6-benzylaminopurine
BF	bright field
CCD	carotenoid cleavage dioxygenase
DW	dry weight
GGPP	geranylgeranyl diphosphate
IAA	indole-3-acetic acid
IPTG	isopropyl β-D-1-thiogalactopyranoside
KT	kinetin
MEP	methylerythritol phosphate
MS	Murashige & Skoog (medium)
MVA	mevalonate
NAA	1-naphthylacetic acid
SD	standard deviation
WT	wild type

Declarations

Ethical approval

Not applicable.

Competing interests.

The authors declare that they have no competing interests.

Supplementary Information

Supplementary Tables S1–S4 and Figures S1–S5 are available in the online version of this article.

Funding.

This work was supported by the Science Foundation of Shaanxi Academy of Sciences (No. 2023K-01), and the Department of Science and Technology of Shaanxi Province (No. 2026JC-YBQN-0237).

Data availability. The data that support the findings of this study are available from the corresponding author upon reasonable request.

Author Contribution

Author contributions. All authors contributed to the study conception and design. Fan Li conducted the foundational experiments and drafted the manuscript. Material preparation was performed by Xu Zhang, Jun Wang, SiNan Chen and YueJuan Zhang. Data collection was performed by XiuLin Han and MengLiang Wen. Data analysis was performed by XiaoWei Gong and Ying Mao. Supervision, conceptualization, review and editing were performed by Yi Wan.

Acknowledgements

We thank Dr. ZhanKu Shi for providing tobacco seeds and Dr. LiJuan Peng for access to the HPLC system. Their support was invaluable to this work.

References

1. Ahrazem O, Rubio-Moraga Á, Berman J (2016) The carotenoid cleavage dioxygenase CCD2 catalysing the synthesis of crocetin in spring crocuses and saffron is a plastidial enzyme. New Phytol 209(2):650–663. https://doi.org/10.1111/nph.13609
2. Chen S, Song X, Zheng Q (2023) The transcription factor SPL13 mediates strigolactone suppression of shoot branching by inhibiting cytokinin synthesis in Solanum lycopersicum. J Exp Bot 74(18):5722. https://doi.org/10.1093/jxb/erad303
3. Dhar MK, Mishra S, Bhat A (2020) Plant carotenoid cleavage oxygenases: structure–function relationships and role in development and metabolism. Brief Funct Genomics 19(1):1–9. https://doi.org/10.1093/bfgp/elz037
4. Dong HW, Wang K, Chang XX (2019) Beta-ionone-inhibited proliferation of breast cancer cells by inhibited COX-2 activity. Arch Toxicol 93(10):2993–3003. https://doi.org/10.1007/s00204-019-02550-2
5. Efferth T (2019) Biotechnology applications of plant callus cultures. Engineering 5(1):50–59. https://doi.org/10.1016/j.eng.2018.11.006
6. Fan L, Gong X, Li Y (2022) Characteristics of a new carotenoid cleavage dioxygenase NtCCD10 derived from Nicotiana tabacum. Planta 256(5). https://doi.org/10.1007/s00425-022-04013-y

7. Fang Q, Li Y, Liu B (2020) Cloning and functional characterization of a carotenoid cleavage dioxygenase 2 gene in safranal and crocin biosynthesis from Freesia hybrida. Plant Physiol Biochem 154:439–450. https://doi.org/10.1016/j.plaphy.2020.06.035
8. Gelvin SB (2003) Agrobacterium-mediated plant transformation: the biology behind the 'gene-jockeying' tool. Microbiol Mol Biol Rev 67(1):16–37. https://doi.org/10.1128/MMBR.67.1.16-37.2003
9. Gong X, Li F, Liang Y (2022) Characteristics of NtCCD1-3 from tobacco, and protein engineering of the CCD1 to enhance β-ionone production in yeast. Front Microbiol 13:1011297. https://doi.org/10.3389/fmicb.2022.1011297
10. Husin M, Hasan M, Taha R (2005) Callus induction from tobacco (Nicotiana tabacum) leaf explants for the production of quinone. https://doi.org/10.1002/apj.5500130506
11. Ke K, Zhang Y, Wang X (2025) Identification, cloning, and functional characterization of carotenoid cleavage dioxygenase (CCD) from Olea europaea and Ipomoea nil. Biology 14(7):752. https://doi.org/10.3390/biology14070752
12. Lalko J, Lapczynski A, McGinty D (2007) Fragrance material review on β-ionone. Food Chem Toxicol. https://doi.org/10.1016/j.fct.2007.09.052
13. Lang J, Pankowski J, Grabarz P (2020) Comparing the effects of different exogenous hormone combinations on seed-derived callus induction in Nicotiana tabacum. Acta Biochim Pol 67(4):449–452. https://doi.org/10.18388/abp.2020_5456
14. Messing SAJ, Gabelli SB, Echeverria I (2010) Structural insights into maize viviparous14, a key enzyme in the biosynthesis of the phytohormone abscisic acid. Plant Cell 22(9):2970–2980. https://doi.org/10.1105/tpc.110.074815
15. Meng N, Yan G-L, Zhang D (2019) Characterization of two Vitis vinifera carotenoid cleavage dioxygenases by heterologous expression in Saccharomyces cerevisiae. Mol Biol Rep 46(6):6311–6323. https://doi.org/10.1007/s11033-019-05072-3
16. Mi J, Jia K-P, Wang JY, Al-Babili S (2018) A rapid LC-MS method for qualitative and quantitative profiling of plant apocarotenoids. Anal Chim Acta 1035:87–95. https://doi.org/10.1016/j.aca.2018.07.002
17. Morote L, Rubio-Moraga Á, López-Jiménez AJ (2023) A carotenoid cleavage dioxygenase 4 from Paulownia tomentosa determines visual and aroma signals in flowers. Plant Sci 329:111609. https://doi.org/10.1016/j.plantsci.2023.111609
18. Nakajima I, Endo M, Haji T (2020) Embryogenic callus induction and Agrobacterium-mediated genetic transformation of 'Shine Muscat' grape. Plant Biotechnol 37(2):185–194. https://doi.org/10.5511/plantbiotechnology.20.0527a
19. Qi Z, Tong X, Zhang Y (2023) Carotenoid cleavage dioxygenase 1 and its application for the production of C13-apocarotenoids in microbial cell factories: a review. J Agric Food Chem 71(49):19240–19254. https://doi.org/10.1021/acs.jafc.3c06459
20. Verma S, Negi NP, Pareek S (2022) Auxin response factors in plant adaptation to drought and salinity stress. Physiol Plant 174(3):e13714. https://doi.org/10.1111/ppl.13714

21. Wang JY, Haider I, Jamil M (2019) The apocarotenoid metabolite zaxinone regulates growth and strigolactone biosynthesis in rice. Nat Commun 10:810. https://doi.org/10.1038/s41467-019-08461-1
22. Werner N, Ramirez-Sarmiento CA, Agosin E (2019) Protein engineering of carotenoid cleavage dioxygenases to optimize β-ionone biosynthesis in yeast cell factories. Food Chem 299:125089. https://doi.org/10.1016/j.foodchem.2019.125089
23. Xinliang L (2023) High frequency callus induction and plant regeneration of Cinnamomum porrectum. J Northeast Forestry Univ. https://doi.org/10.13759/j.cnki.dlxb.2023.03.022
24. Yi F, Song A, Cheng K (2023) Strigolactones positively regulate Verticillium wilt resistance in cotton via crosstalk with other hormones. Plant Physiol 192(2):945–966. https://doi.org/10.1093/plphys/kiad053
25. Yoo HJ, Chung MY, Lee HA (2023) Natural overexpression of carotenoid cleavage dioxygenases 4 in tomato alters carotenoid flux. Plant Physiol 192(2):1289–1306. https://doi.org/10.1093/plphys/kiad049
26. Zhang C, Chen X, Lindley ND (2018) A plug-n-play modular metabolic system for the production of apocarotenoids. Biotechnol Bioeng 115(1):174–183. https://doi.org/10.1002/bit.26462
27. Zhong Y, Pan X, Wang R (2020) ZmCCD10a encodes a distinct type of carotenoid cleavage dioxygenase and enhances plant tolerance to low phosphate. Plant Physiol 184(1):374. https://doi.org/10.1104/pp.20.00378
28. Paine JA, Shipton CA, Chaggar S (2005) Improving the nutritional value of Golden Rice through increased pro-vitamin A content. Nat Biotechnol 23(4):482–487. https://doi.org/10.1038/nbt1082
29. Rao SR, Ravishankar GA (2002) Plant cell cultures: chemical factories of secondary metabolites. Biotechnol Adv 20(2):101–153. https://doi.org/10.1016/S0734-9750(02)00007-1
30. Roberts SC (2007) Production and engineering of terpenoids in plant cell culture. Nat Chem Biol 3(7):387–395. https://doi.org/10.1038/nchembio.2007.8
31. Wilson SA, Roberts SC (2012) Recent advances towards development and commercialization of plant cell culture processes for the synthesis of biomolecules. Plant Biotechnol J 10(3):249–268. https://doi.org/10.1111/j.1467-7652.2011.00664.x

Figures

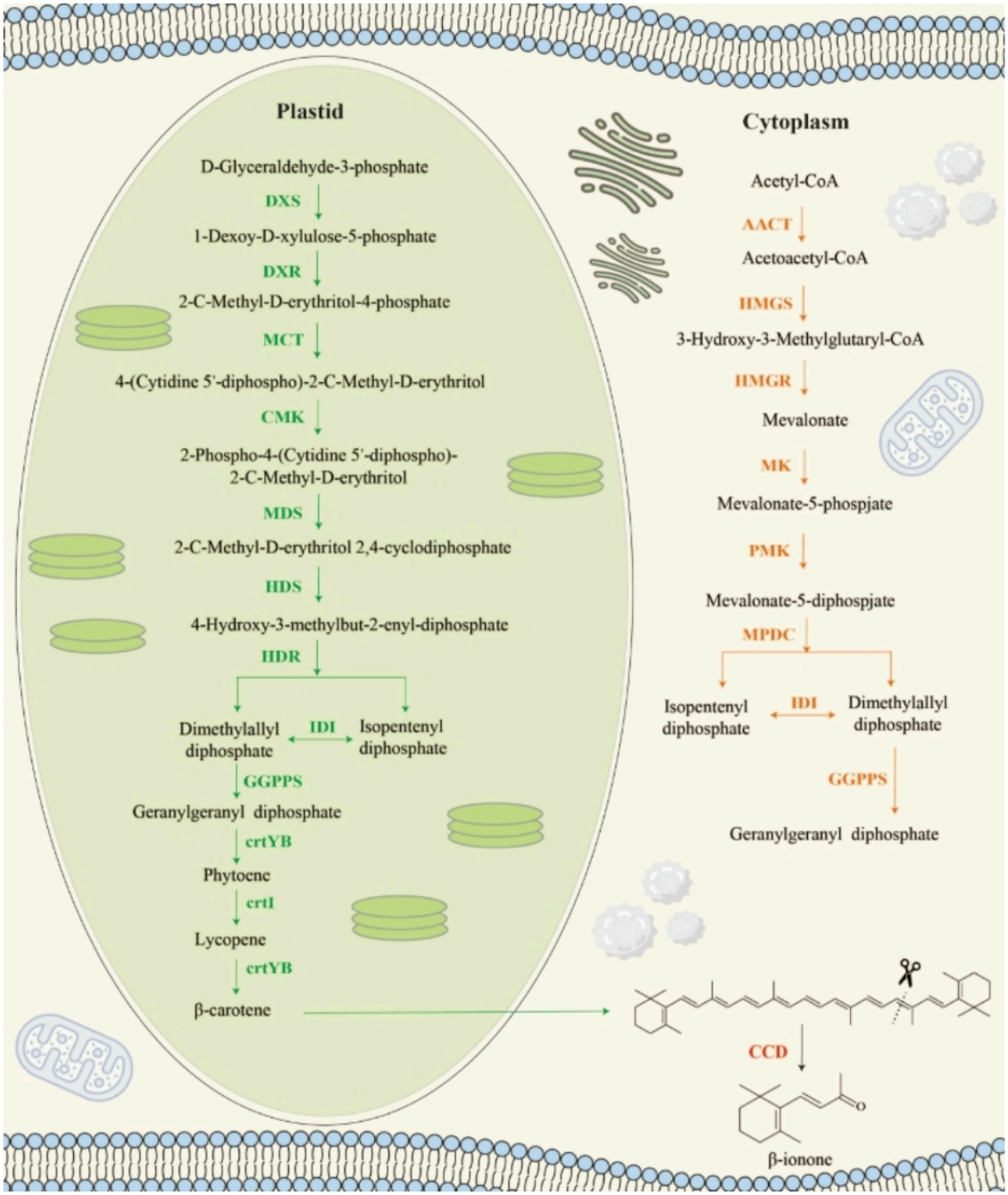

Figure 1

The β-ionone metabolic pathway in plant cells. MVA, mevalonate pathway; DXS, 1-deoxy-D-xylulose 5-phosphate synthase; DXR, 1-deoxy-D-xylulose 5-phosphate reductoisomerase; MCT, 4-diphosphocytidyl-2-C-methyl-D-erythritol synthase; CMK, 4-diphosphocytidyl-2-C-methyl-D-erythritol kinase; MDS, 2-C-methyl-D-erythritol 2,4-cyclodiphosphate synthase; HDS, 1-hydroxy-2-methyl-2-(E)-butenyl 4-diphosphate synthase; HDR, 4-hydroxy-3-methylbut-2-enyl diphosphate reductase; IDI, isopentenyl diphosphate

isomerase; GPPS, geranyl diphosphate synthase; GGPPS, geranylgeranyl diphosphate synthase; crtE, geranylgeranyl diphosphate synthase; crtYB, phytoene synthase and cyclase; crtI, phytoene desaturase; CCD, carotenoid cleavage dioxygenase; MEP, methylerythritol phosphate; HMGS, hydroxymethylglutaryl-CoA synthase; HMGR, hydroxymethylglutaryl-CoA reductase; MK, mevalonate kinase; PMK, phosphomevalonate kinase; MPDC, mevalonate pyrophosphate decarboxylase. (B) The CCD subfamilies and their metabolites.

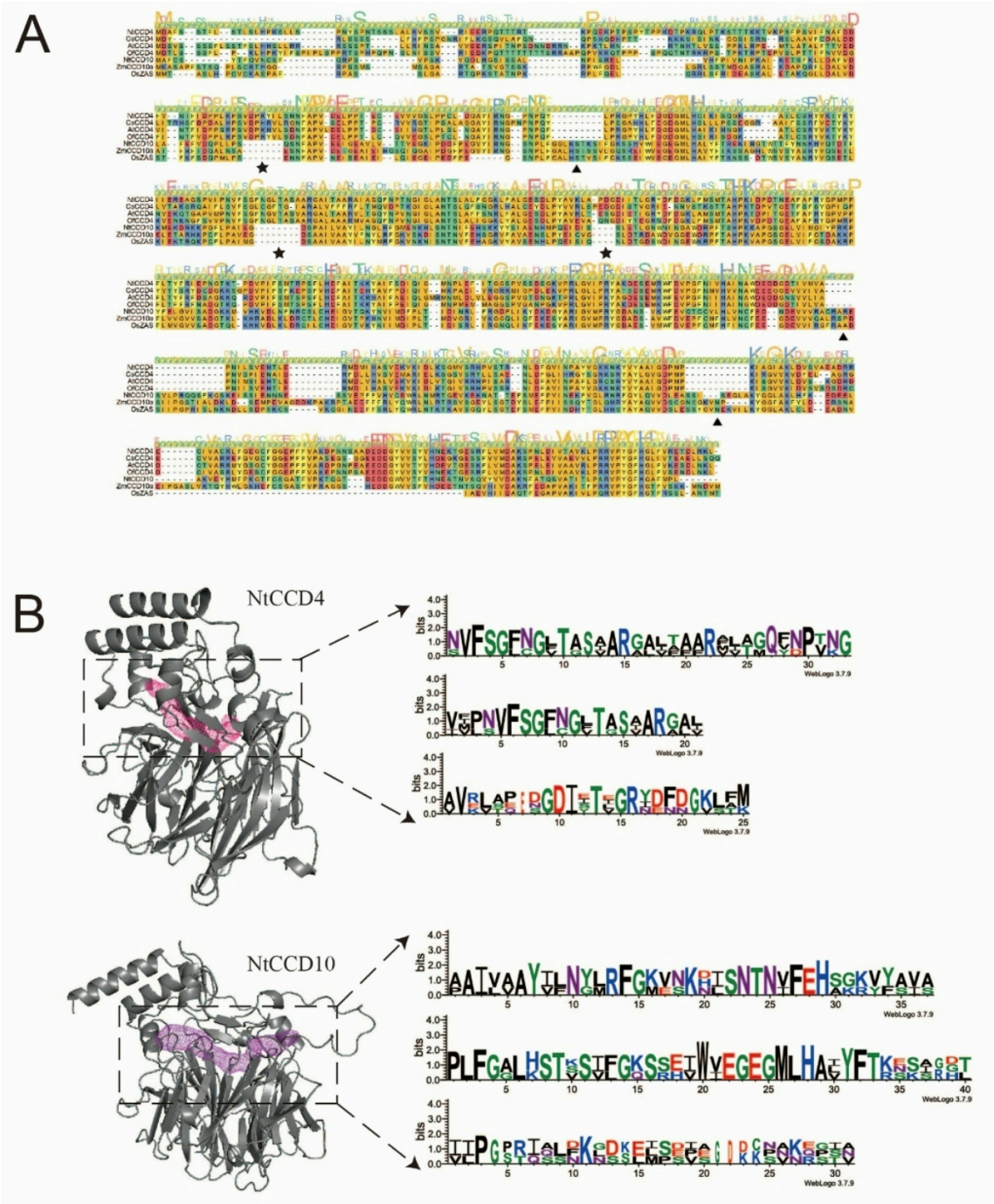

Figure 2

The differences in sequences and structures between NtCCD4 and NtCCD10. (A) CCD amino-acid sequence alignment. Black stars mark the unique sequence of the CCD4 subfamily; black triangles mark the specific sequences of the CCD10 subfamily. (B) Differences in protein structure, substrate channels and motifs between NtCCD4 and NtCCD10. Rose-red and purple grids represent protein substrate channels.

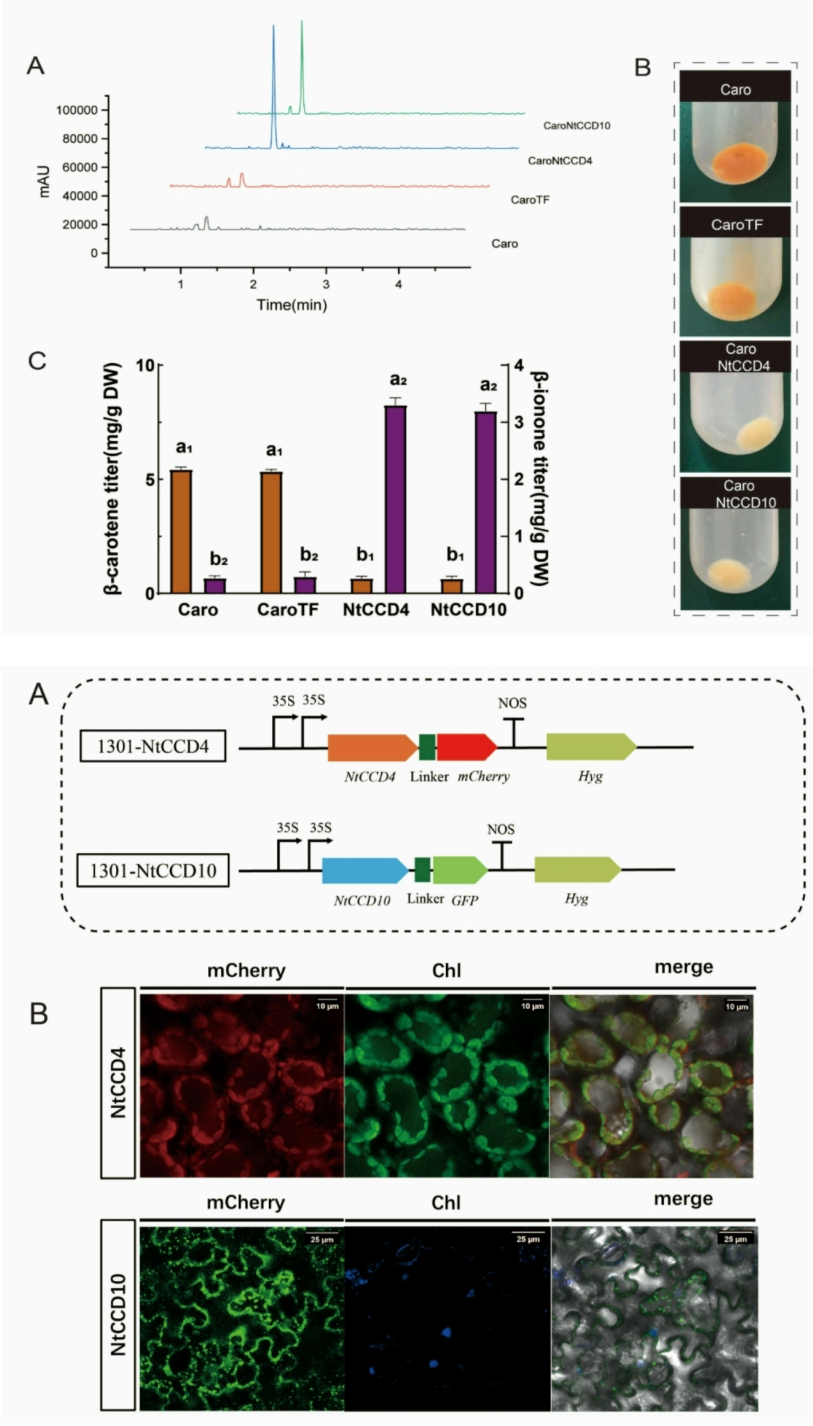

Figure 3

Detection of β-carotene accumulation and β-ionone production in E. coli. (A) Detection of β-ionone in E. coli by UPLC. (B) Colour variation of E. coli strains. (C) β-Carotene and β-ionone production in E. coli. Quantification was performed via external standard curves. Data are means ± SD (n = 3 biological replicates). Bars labelled with different lowercase letters indicate significant differences (P < 0.001).

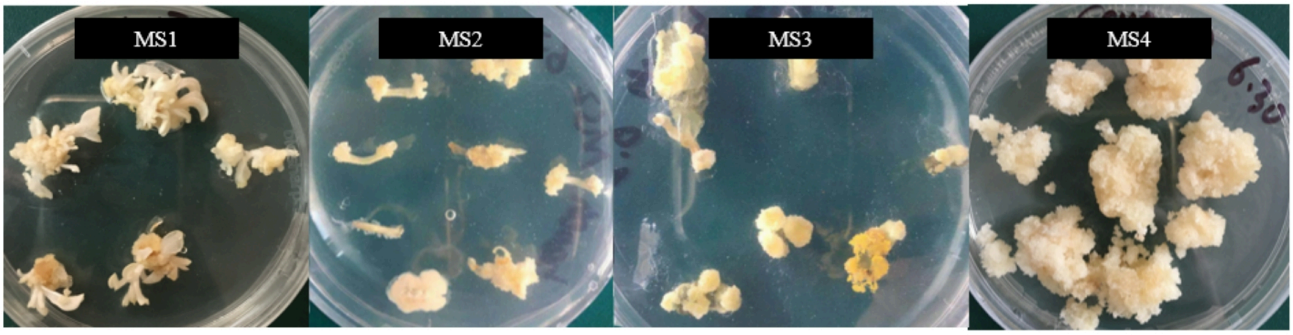

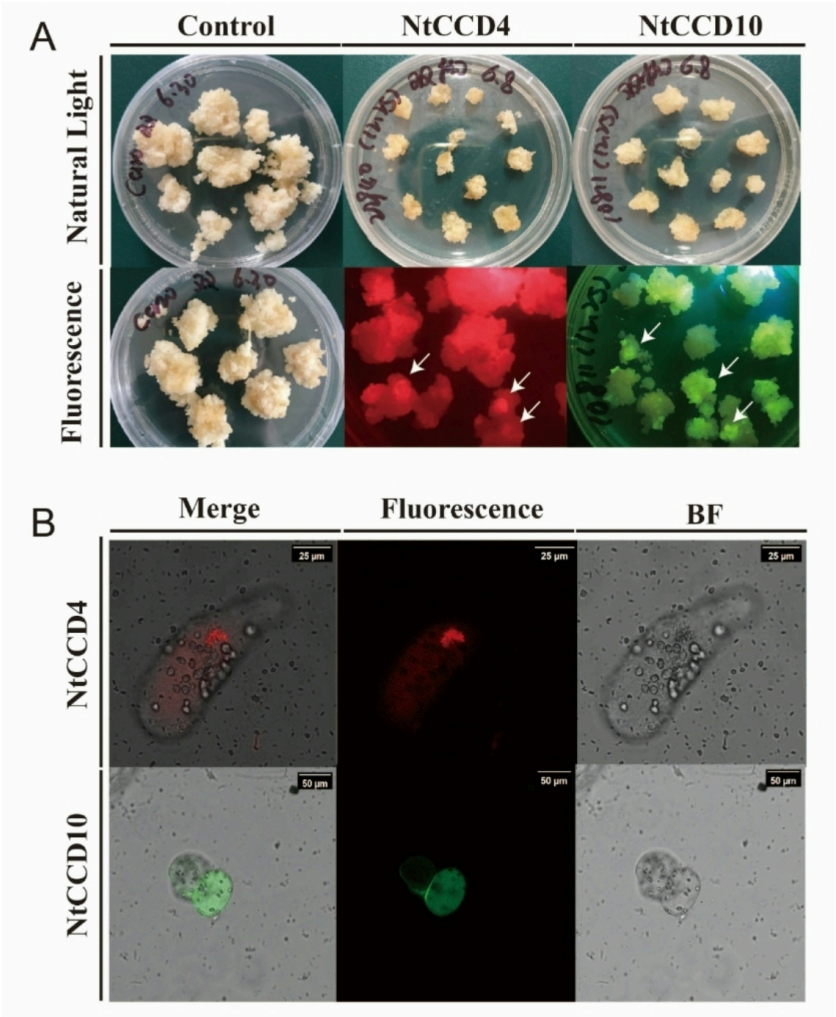

Figure 4

Schematic diagram of the construction of NtCCD4 and NtCCD10 plant expression vectors. (A) Schematic diagrams of the NtCCD4 and NtCCD10 plant expression vector constructs. (B) Subcellular localization of NtCCD4 and NtCCD10 in N. benthamiana. mCherry is shown in red; Chl is chloroplast autofluorescence; mCherry and Chl were merged. GFP is shown in green; nuclei were stained with DAPI; GFP and DAPI were merged.

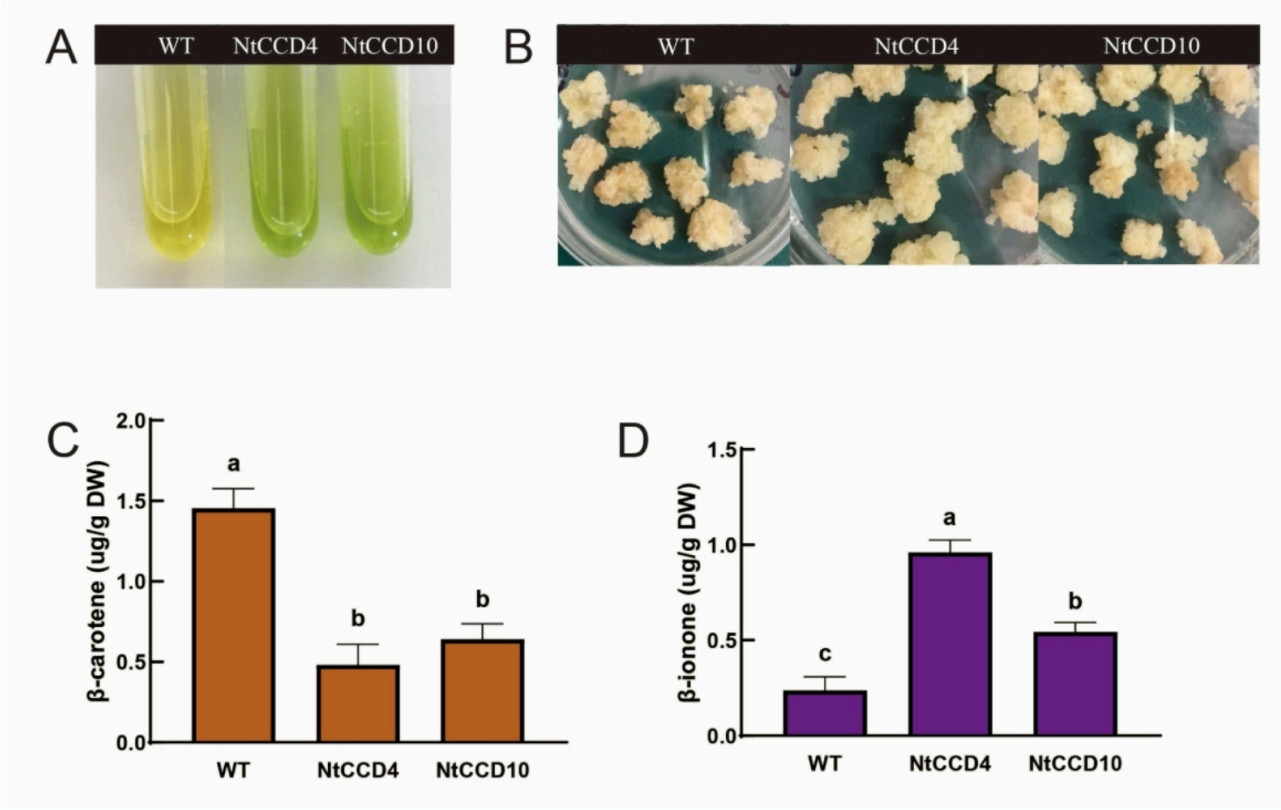

Figure 5

Effects of tobacco callus induction on different induction media.

Supplementary Files

This is a list of supplementary files associated with this preprint. Click to download.

- PCTOCSupplementaryinformation.docx